Motivation

The 3D in situ stress state is an important field variable to assess the reactivation potential of tectonic faults and to predict the future structural evolution over geological time spans. Furthermore, it is a critical parameter for a wide range of underground engineering activities addressing questions with respect to stability aspects as well as productivity for georeservoirs [*Fuchs and Müller*, 2001; *Moeck and Backers*, 2011]. Stability refers e.g. for safe drill path, long-term stability of nuclear waste disposal sites or CO_2 sequestration in the underground. For the depletion of georeservoirs, re-injection of waste water and hydraulic fracturing to enhance permeability, the in situ stress is critical as it determines how much stress changes the reservoir can sustain before e.g. sealing faults are reactivated or cap rock integrity is affected. Knowledge of the in situ stress state is also required in order to forecast the effectiveness of hydraulic fracturing performed to enhance the permeability and thus productivity.

However, data of the in situ stress are in general very sparse and incomplete as only a subset of the six components of the 3D stress tensor is available. E.g. the World Stress Map (WSM) Project compiles globally the contemporary orientation of maximum horizontal stress S_H, but it has only 21,750 data records in the upper 40 km [*Heidbach et al.*, 2010]. A compilation of stress magnitude data is in progress, but the global dataset has so far only ~1200 data records [*Zang et al.*, 2012]. In order to determine all components of the 3D stress tensor spatially continuous, a geomechanical-numerical model has to be set up and calibrated against the stress information.

We present here a completely revised compilation of stress data for Switzerland and a 3D semi-generic geomechanical-numerical model of a small area in Northern Switzerland that provides a spatially continuous description of the 3D stress tensor and its variability. In particular, we investigate by means of the model to what extent pre-existing major fault structures and stiffness contrasts among the various sediment layers of the Mesozoic sediments influence in situ stress. We give an overview of the stress data and the stress pattern in Switzerland and then show the model and a few key results.

Stress state in Switzerland

As part of the Sectoral Plan Deep Geological Repositories, all stress data for Switzerland and adjacent regions from the World Stress Map database release 2008 were re-assessed, updated and new data records were added. This resulting revised data set contains 107 new data records. 15 data records from 11 new boreholes with up to 2.5 km depth as well as re-analysis of seven old Nagra boreholes provide a consistent data set that is evaluated with common criteria according to the latest WSM quality ranking scheme (Heidbach et al., 2010). In total the dataset for Switzerland and adjacent regions has now 567 data records with 289 of them having reliable A-C quality [*Heidbach and Reinecker, 2013*].

The overall stress pattern of Switzerland shows a long wave-length trend with a mean S_H orientation of 155 ± 30°. Northeast of Lake Constance S_H is N-S oriented and rotates gradually counter-clockwise by ~ 40° along the alpine front from East to West to a NW-SE orientation in west Switzerland in agreement with earlier findings [*Reinecker et al.*, 2010]. S_H is oriented perpendicular to the gradient of the Alps, the Moho and the basement and sub-parallel to the indentation direction of the Adriatic plate with Eurasia. These large-scale density contrasts and are the key control of the stress pattern in Northern Switzerland. Here the mean S_H orientation is 160 ± 21° and it is oriented almost perpendicular to the bounding faults of the Permian-Carboniferous Trough (Figure 1). Therefore, a reactivation in normal or strike-slip faulting is unlikely. In contrast, S_H is oriented approximately 30-50° to the hercynian and rheinish striking faults. In the upper 7-8 km strike-slip is prevailing whereas at greater depth normal faulting is the major faulting mechanism.

The regional trend of the stress pattern and the mean S_H orientation is independent from the chosen sub datasets and shows no general difference when e.g. data records only from the basement or sediments are taken into account. Changes of the mean values in the order of 10-15° are statistically not significant as standard deviation of the mean S_H orientation of the data is in the order of 15-25°.

Thus, the spatial variation of the S_H orientation does not support the hypothesis of a possible detachment horizon. However, the missing S_H rotation at larger scale does not necessarily imply that a mechanical decoupling is not effective for two reasons: (1) Assuming that the S_H orientation is driven from the same far-field processes a mechanical decoupling would certainly result in a substantial changes of the horizontal stress magnitudes with depth, but the S_H orientation can be unaffected. (2) A few individual boreholes have a significantly rotation of the S_H orientation with depth indicating that at least locally a mechanical decoupling occurs. Finally, the question whether a detachment is still mechanically active or not and to what spatial extend this mechanism occurs cannot be answered with the stress data.

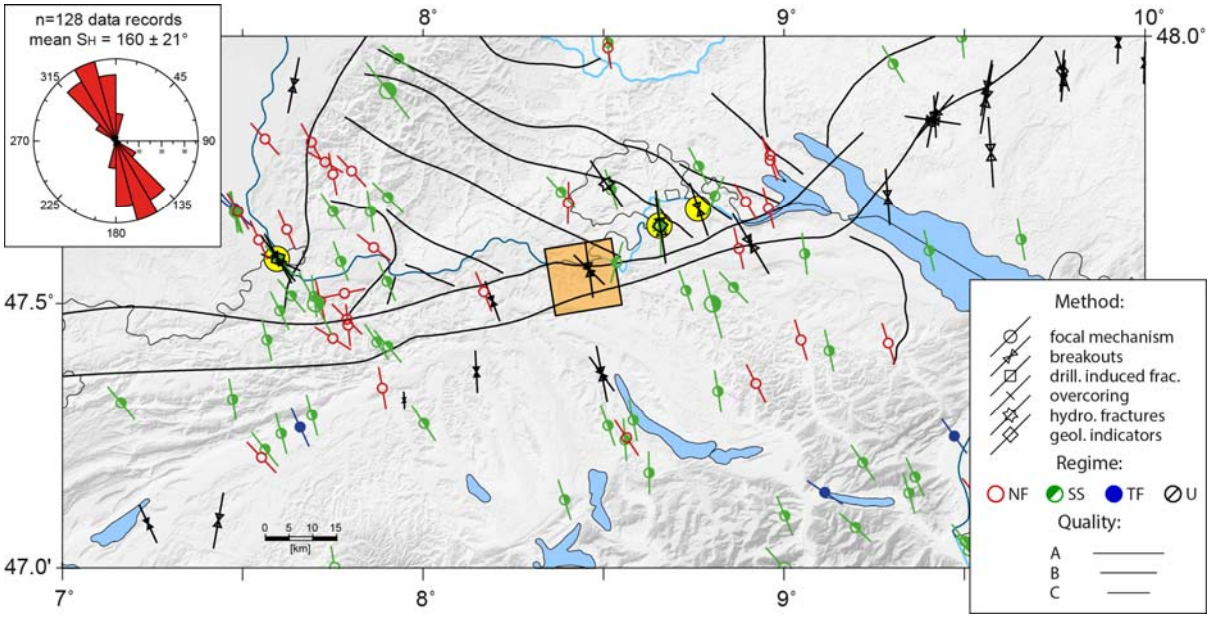

Figure.1. *Stress map of northern Switzerland based on A-C quality data records of the revised WSM database release 2008 [Heidbach and Reinecker, 2013]. Bars indicate the S_H orientation and symbols the stress indicator; bar length is proportional to data quality. Colours indicate tectonic regime with red for normal faulting (NF), green for strike-slip faulting (SS), blue for thrust faulting (TF), and black for unknown regime (U). Bold lines denote the major faults, yellow circles the three sites where stress magnitude data are available (Basel, Benken, Schlattingen from W to E) and the orange square is the area of the geomechanical-numerical model presented in Fig 2. The rose diagram shows the S_H orientations from the 128 data records displayed; the mean S_H orientation is 160 ± 21°. The standard deviation is quality- weighted and determined with the statistics of bi-modal data.*

3D semi-generic geomechanical-numerical model

The key goal of the geomechanical-numerical model is to quantify the spatially continuous 3D in situ stress in the $14 \times 14 \times 3$ km^3 sub-volume (Figure 1). However, the available stress data within the model area is limited to the S_H orientation data from the Weiach borehole and no stress magnitude data are available for the model calibration. Thus, the model has, even though its geometry resembles the geological setting of that region, to some extend a generic character to a certain extend. Instead we are using stress magnitude data from hydrofracs of the Benken borehole that is at ~ 20 km distance to the model area. Thus, the absolute stress values from the model are potentially deviating from the real stress state, but the impact of various stress controlling factors can still be studied quantitatively in terms of the their relative importance. In particular, we want to study the influence of pre-existing faults and lithological formations with different stiffness on the spatial variability of the stress state.

We assume for the model that transient (earthquake cycle, sedimentation, erosion etc.) and man-made processes can be neglected and thus only the contributions from gravity and tectonic stresses from past and on-going tectonic processes are considered. Our workflow encompasses four consecutive steps: (1) Construction of the 3D model geometry from surface mapping, borehole and seismic data. In particular, the geometry includes the boundaries between mechanically significant stratigraphic

formations, topography and the major faults (Figure 2 and Figure 3a). The model is discretized into ~270.000 linear hexaeder elements (Figure 2). We attribute to each formation the elasto-plastic properties and density. Additionally, the two implemented faults that cut the model in roughly E-W direction, have an effective friction of μ=0.2. (2) Determination of an appropriate initial stress state that is in equilibrium with gravity and application of displacement boundary conditions to impose the tectonic stresses from the geological history. The solution of the partial differential equation is solved numerically with the finite element software Abaqus; the 3D geometry and the 3D finite element mesh is constructed with gOcad and HyperMesh, respectively. (3) Calibration of the modelled stress field against model-independent data such as S_H orientations, the prevailing tectonic regime, and stress magnitude data (here we use the aforementioned hydrofrac data from Benken, see figure 1). (4) After a satisfying fit to the model-independent constraints the analysis of the model sensitivity due to the uncertainties of the free model parameters can be performed as well as sensitivity tests with respect to fault properties (effective friction coefficient), uncertainties in the rock properties and the initial stress state of the model. For the 3D vizualisation we use Tecplot 360 with an own geoscientific add-on.

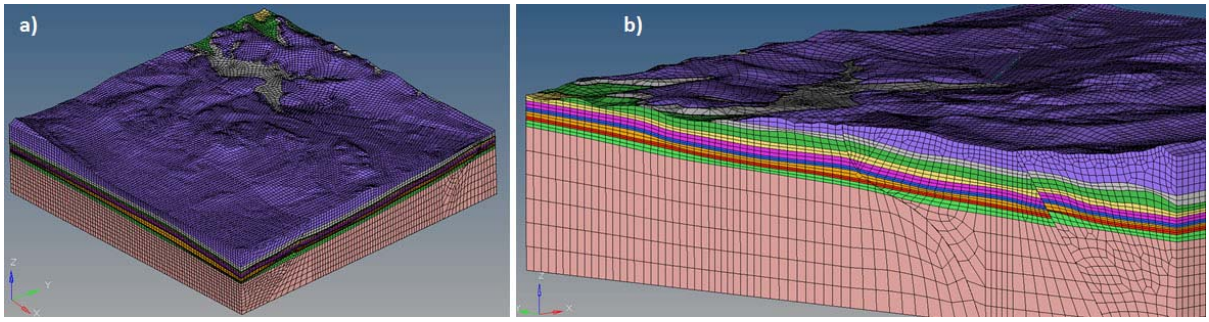

Figure 2. *Finite element mesh of the 3D model. a) View from SE to NW downward, b) Western model boundary, view to NE; Mesozoic formations become shallower from south to north. Formations are from top to bottom: Molasse, oberer Malm, Effinger layers, oberer Dogger, Opalinus Clay, Keuper, Gipskeuper, oberer Muschelkalk, mittlerer Muschelkalk, Permocarboniferous/basement.*

Figure 3 shows N-S profiles of the modelled stratigraphic formations and the best fit model result in terms of the total stress ratios S_H/S_h, S_H/S_V and S_h/S_V with S_h being the minimum horizontal stress and S_V being the vertical stress, respectively. Best fit means that the model has a tectonic regime close to strike-slip as indicated by the shallow stress data, that the S_H orientation of the model is between 165-175°N, which is in agreement with data from Weiach at depth between 560-2100 m (S_H orientation is 173 ± 15°) and that we meet the ratio of S_h/S_v from data of the borehole in Benken.

We find large deviations of the ratio S_H/S_h between the different formations above the basement. In the relatively weak Opalinus Clay S_H/S_h is in the range of 1.2-1.4, whereas in the competent Malm formation above k varies between 1.7 and 1.9. These values are in general agreement with findings in Dogger and Oxfordian formations investigated in the rock laboratory at Bure, France [*Wileveau et al.*, 2007]. This is an expression of the marked contrasts in stiffness and strength of these formations.

Conclusions

The results shows that even sparse, point-wise and incomplete information of the stress tensor are sufficient to model the relative local variability of the 3D stress tensor and in particular to study the impact of strength and stiffness contrasts as well as faults on the stress field. However, the reliability modelled absolute 3D in situ stress strongly depends on three key aspects, (1) a reliable 3D geological model as major pre-existing faults have a local impact on in situ stress, (2) knowledge of the elasto-plastic material properties as these can change in situ stress significantly and (3) stress magnitude data to calibrate the initial stress state of the model. Even though our model seems to resemble stress ratios that have been measured in other settings, there is no guarantee that this is true for the region investigated. A final validation of the model is only possible with stress magnitude data from within the model area that are representative for a larger area.

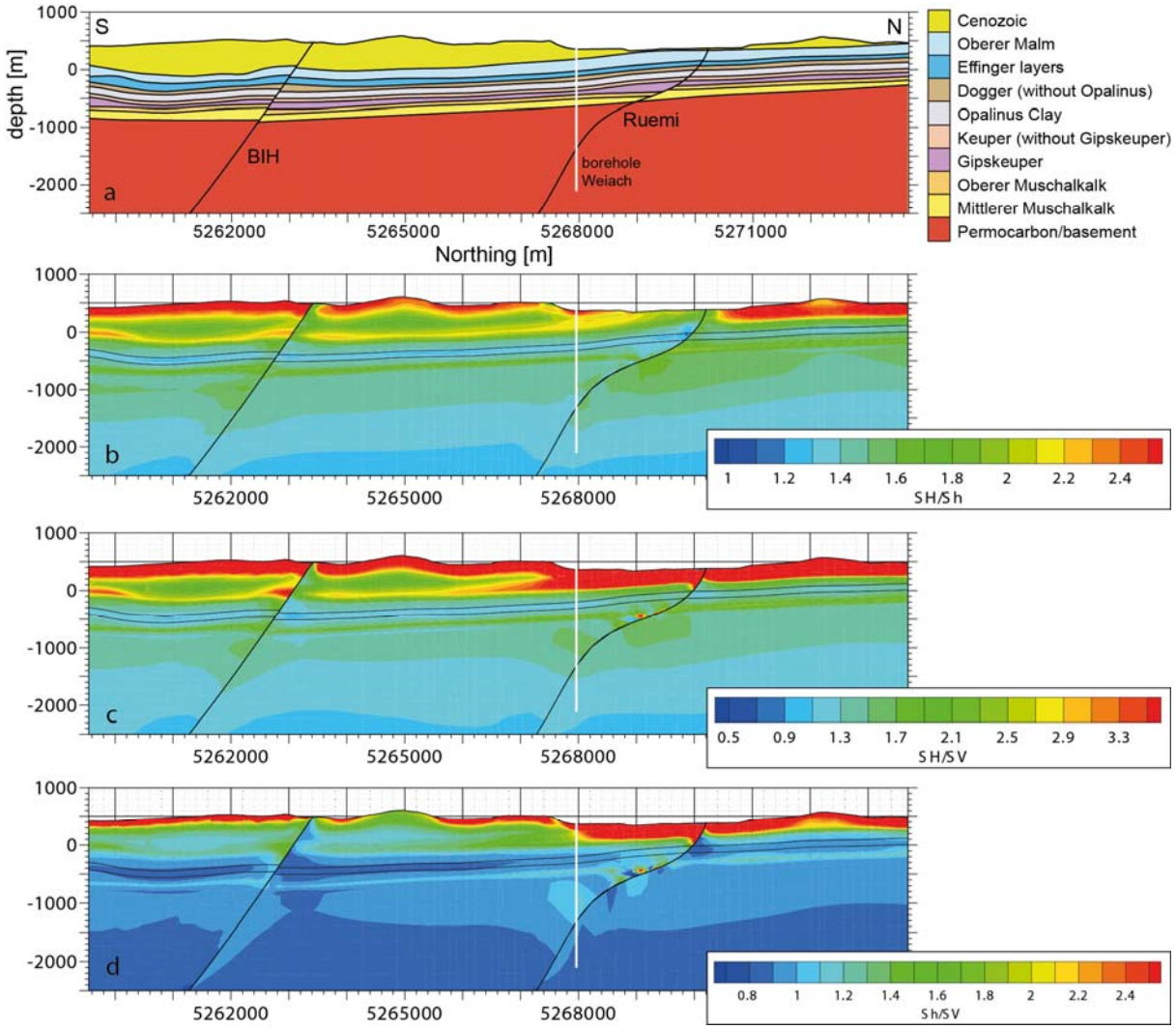

Figure 3. *NS-Profiles through the centre of the best fit model with a) stratigraphy, b) S_H/S_h ratio, c) S_H/S_V ratio and d) S_h/S_V ratio. Thin black lines in b)-d) denote the top and bottom of the Opalinus Clay. Note the contrasting total stress ratios of Opalinus Clay with other formations.*

References

Fuchs, K., and B. Müller (2001), World Stress Map of the Earth: a key to tectonic processes and technological applications, *Naturwissenschaften*, *88*, 357-371.

Heidbach, O., M. Tingay, A. Barth, J. Reinecker, D. Kurfeß, and B. Müller (2010), Global crustal stress pattern based on the World Stress Map database release 2008, *Tectonophysics*, *462*(1-4), doi:10.1016/j.tecto.2009.1007.1023.

Moeck, I., and T. Backers (2011), Fault reactivation potential as a critical factor during reservoir stimulation, *First Break*, *29*(doi: 10.3997/1365-2397.2011014), 73-80.

Heidbach, O. and J. Reinecker (2013), Analyse des rezenten Spannungsfelds der Nordschweiz, Nagra Arb. Ber. NAB 12-05, 120 pp.

Reinecker, J., M. Tingay, B. Müller, and O. Heidbach (2010), Present-day stress orientation in the Molasse Basin, *Tectonophysics*, *462*(1-4), doi:10.1016/j.tecto.2009.1007.1021.

Wileveau, Y., F. H. Cornet, J. Desroches, and P. Blumling (2007), Complete in situ stress determination in an argillite sedimentary formation, *Phys. Chem. Earth*, *32*, doi: 10.1016/j.pce.2006.1003.1018, 1866-1878.

Zang, A., O. Stephansson, O. Heidbach, and S. Janouschkowetz (2012), World Stress Map Database as a Resource of Rock Mechanics and Rock Engineering, *Geotech. Geol. Eng.*, doi 10.1007/s10706-10012-19505-10706.